RAA 2017 Vol. **17** No. **1**, 3 (10pp) doi: 10.1088/1674–4527/17/1/3

http://www.raa-journal.org *http://iopscience.iop.org/raa*

***R**esearch in*
***A**stronomy and*
***A**strophysics*

Chaos-induced resistivity of collisionless magnetic reconnection in the presence of a guide field

Meng Shang[1,2], De-Jin Wu[1], Ling Chen[1] and Peng-Fei Chen[3,4]

[1] Key Laboratory of Planetary Sciences, Purple Mountain Observatory, CAS, Nanjing 210008, China; *djwu@pmo.ac.cn*
[2] University of Chinese Academy of Sciences, Beijing 100049, China
[3] School of Astronomy and Space Science, Nanjing University, Nanjing 210023, China
[4] Key Lab of Modern Astron. and Astrophys., Nanjing University, Nanjing 210023, China

Received 2016 May 17; accepted 2016 September 13

Abstract One of the most puzzling problems in astrophysics is to understand the anomalous resistivity in collisionless magnetic reconnection that is believed extensively to be responsible for the energy release in various eruptive phenomena. The magnetic null point in the reconnecting current sheet, acting as a scattering center, can lead to chaotic motions of particles in the current sheet, which is one of the possible mechanisms for anomalous resistivity and is called chaos-induced resistivity. In many interesting cases, however, instead of the magnetic null point, there is a nonzero magnetic field perpendicular to the merging field lines, usually called the guide field, whose effect on chaos-induced resistivity has been an open problem. By use of the test particle simulation method and statistical analysis, we investigate chaos-induced resistivity in the presence of a constant guide field. The characteristics of particle motion in the reconnecting region, in particular, the chaotic behavior of particle orbits and evolving statistical features, are analyzed. The results show that as the guide field increases, the radius of the chaos region increases and the Lyapunov index decreases. However, the effective collision frequency, and hence the chaos-induced resistivity, reach their peak values when the guide field approaches half of the characteristic strength of the reconnection magnetic field. The presence of a guide field can significantly influence the chaos of the particle orbits and hence the chaos-induced resistivity in the reconnection sheet, which decides the collisionless reconnection rate. The present result is helpful for us to understand the microphysics of anomalous resistivity in collisionless reconnection with a guide field.

Key words: magnetic reconnection — plasmas — chaos — Sun: flares

1 INTRODUCTION

Magnetic reconnection (Dungey 1958; Giovanelli 1946), an effective mechanism of magnetic energy release, has been believed widely to play an important and key role in various eruptive phenomena such as terrestrial aurorae (Dungey 1961), solar flares (Parker 1957; Sweet 1958) and γ-ray bursts (Lyutikov 2006). In the theory of magnetohydrodynamics (MHD), the evolution of the magnetic field $\boldsymbol{B}$ can be determined by the so-called magnetic induction equation as follows

$$\frac{\partial \boldsymbol{B}}{\partial t} = \nabla \times (\boldsymbol{U} \times \boldsymbol{B}) - \nu_{\rm m} \nabla \times (\nabla \times \boldsymbol{B}) \,, \quad (1)$$

where $\boldsymbol{U}$ is the plasma flow velocity, $\nu_{\rm m} = \eta/\mu_0$ is the magnetic diffusivity coefficient (also called the magnetic viscosity coefficient), η is the plasma resistivity and μ_0 is the vacuum permeability. On the right hand side of the above equation, the first and second terms represent the magnetic convection due to plasma flow ($\propto \boldsymbol{U}$) and the magnetic dissipation due to plasma resistivity ($\propto \eta$), respectively.

An effective release of magnetic energy into kinetic energy of the plasma particles requires a sufficiently high resistivity η. For the case of solar flares, a typical releasing time scale is $\tau \sim 10^3$ s, implying the magnetic diffusivity $\nu_{\rm m} \sim L^2/\tau \sim 10^{11}\,{\rm m^2\,s^{-1}}$ for an inhomogeneity scale $L \sim 10^7$ m of the magnetic field. However,

the magnetic diffusivity coefficient, caused by classical Spitzer resistivity (Spitzer 1956)

$$\eta = \frac{m_{\rm e}\nu_{\rm ei}}{ne^2}, \tag{2}$$

$\nu_{\rm m} = \eta/\mu_0$ is typically of the order $1\,{\rm m}^2\,{\rm s}^{-1}$ for the characteristic plasma temperature $T \sim 10^6\,{\rm K}$ and density $n \sim 10^9\ {\rm cm}^{-3}$ in the lower solar corona. This is much less than the above magnetic diffusivity coefficient required by the effective magnetic energy release during solar flares, where e is the elementary charge, $m_{\rm e}$ and n are the electron mass and density, respectively, and $\nu_{\rm ei}$ is the Coulomb collision frequency between electrons and ions. Such an inconsistency has motivated extensive interest to explore various mechanisms of producing non-collisional resistivity, also called anomalous resistivity, such as the lower-hybrid drift wave (Huba et al. 1980), small-amplitude MHD fluctuations (Boozer 1986), the electron MHD effect (Bulanov et al. 1992), the Hall effect controlled by ion inertia (Biskamp et al. 1995) and the mixing effect of dynamical chaos of particle orbits (Yoshida et al. 1998; Egedal & Fasoli 2001).

In the neighborhood of the magnetic null point, it is possible that the spatial inhomogeneity of electromagnetic fields causes enough strong nonlinearity in the motion equation of charged particles to result in chaotic motions of the particles (Grad & Van Norton 1962, Schmidt 1962). The mixing effect of chaotic motions increases the kinetic entropy of the system that consists of current-carrying charged particles in the reconnection current sheet, and yields efficient heating of plasma in the reconnection region (Horton et al. 1991; Yoshida et al. 1998; Egedal & Fasoli 2001). In particular, Numata & Yoshida (2002, 2003) pointed out that, in an open system with the convection of particles into and out of the reconnection region, the continuous dissipation can be carried out and that the resulting chaos-induced resistivity may explain the necessary anomalous resistivity leading to a fast magnetic reconnection.

Although magnetic reconnection is commonly considered as a basically two-dimensional process in which oppositely directed magnetic field lines merge with each other, it is possible that in many interesting cases the ambient magnetic field still has a surviving non-zero component perpendicular to the merging field lines. This surviving field is usually termed the guide field (Ricci et al. 2004, Fitzpatrick & Porcelli 2004). Without doubt, the presence of a guide field considerably changes the dynamical characteristics of particle orbits in the reconnection region (Liu et al. 2009). Following Numata & Yoshida (2002, 2003), this paper investigates the chaos-induced resistivity in the presence of a constant guide field. The result implies that the presence of a guide field indeed influences significantly the chaos of the particle orbits and hence the chaos-induced resistivity in the reconnection region.

The remainder of this paper is organized as follows. The basic model is described in Section 2, and the chaotic behavior of individual particle dynamics is discussed in Section 3. The multi-particle statistical characteristics and the effective resistivity in a current sheet are further analyzed in Section 4. Finally, summary and conclusion are presented in Section 5.

2 BASIC PHYSICS MODEL

For the sake of simplicity, we take a two-dimensional X-shaped field (the degenerate case of a Y-shaped field) in the x-y plane of a Cartesian rectangular coordinate system ($\boldsymbol{r} = (x,\ y,\ z)$) as the reconnection field and a uniform field along the z axis as the guide field (see Fig. 1), which is represented by

$$\boldsymbol{B} = \left(\frac{y}{R_0},\ \frac{x}{R_0},\ \delta\right) B_0, \tag{3}$$

where B_0 is the characteristic strength of the reconnection magnetic field, R_0 the characteristic scale of the magnetic field variation and δ the dimensionless measurement of the guide field strength in the unit of B_0. In addition, a constant electric field along the guide magnetic field is given by

$$\boldsymbol{E} = (0,\ 0,\ E_z)\,, \tag{4}$$

where E_z is the constant electric field.

The collisionless motion of a charged particle with mass m and charge q is controlled by the motion equations as follows

$$\begin{aligned} \frac{d\boldsymbol{r}}{dt} &= \boldsymbol{v}, \\ \frac{d\boldsymbol{v}}{dt} &= \frac{q}{m}\left(\boldsymbol{E} + \boldsymbol{v}\times\boldsymbol{B}\right), \end{aligned} \tag{5}$$

where $\boldsymbol{E}$ and $\boldsymbol{B}$ are the electric and magnetic fields in Equations (4) and (3), respectively. For the sake of convenience, we normalize the spatial and temporal variables by R_0 and $\tau_{\rm A} \equiv R_0/v_{\rm A}$, respectively, where $v_{\rm A}$ is the Alfvén velocity corresponding to the characteristic strength of the magnetic field B_0. The electric and magnetic fields are normalized by $M_{\rm A}v_{\rm A}B_0$ and B_0, respectively, where $M_{\rm A} = E_z/\left(v_{\rm A}B_0\right)$ is the Alfvén Mach number of the electric drift velocity $\boldsymbol{v}_{\rm E} = \boldsymbol{E}\times\mathbf{B}/B^2$. Thus, the dimensionless form of Equation (5) reads as:

$$\begin{aligned} \frac{d\boldsymbol{r}'}{dt'} &= \boldsymbol{v}', \\ \frac{d\boldsymbol{v}'}{dt'} &= \frac{R_0}{\lambda_{\rm c}}\left(M_{\rm A}\boldsymbol{E}' + \boldsymbol{v}'\times\boldsymbol{B}'\right), \end{aligned} \tag{6}$$

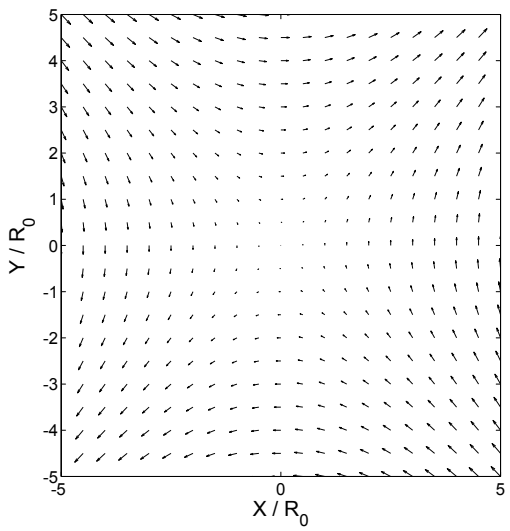

Fig. 1 X-shaped magnetic field in the reconnection region, where R_0 is the characteristic scale of the magnetic field variation.

where the variables with the superscript "$\prime$" are dimensionless forms of the corresponding variables, $\lambda_{\rm c} \equiv v_{\rm A}/\omega_{\rm c}$ is the collisionless skin depth of the charged particles and $\omega_{\rm c} \equiv qB_0/m$ is the characteristic gyrofrequency with the sign of the charge q (i.e., $\omega_{\rm c}$ is positive and negative for ions and electrons, respectively). In addition, the dimensionless electric and magnetic fields in Equations (4) and (3) are given by,

$$\boldsymbol{E}' = (0,\ 0,\ 1) \tag{7}$$

and

$$\boldsymbol{B}' = (y',\ x',\ \delta)\,. \tag{8}$$

In the above equations the parameters $\lambda_{\rm c}$ and $\omega_{\rm c}^{-1}$ are the characteristic spatial and temporal scales of individual particles, in which the kinetic effect plays an important role. In particular, when the inhomogeneity scale of the field R_0 is much larger than the kinetic scale of particles $\lambda_{\rm c}$ (i.e., $R_0 \gg \lambda_{\rm c}$), the long-term average motion orbit ($t \gg \omega_{\rm c}^{-1}$) is dominated by the flow drift velocity $\boldsymbol{v}_{\rm E}$. However, when $R_0 \sim \lambda_{\rm c}$ strong inhomogeneity in the reconnection region leads to substantial deviation of the particle motion from the flow drift motion described mainly by $\boldsymbol{v}_{\rm E}$ and results in chaotic orbits.

3 CHAOTIC BEHAVIOR OF INDIVIDUAL PARTICLE ORBITS

Motion associated with orbits of charged particles with mass m and charge q in the electromagnetic field described by Equations (7) and (8) can be calculated numerically by Equation (6). To stress the importance of chaotic orbits, we take $R_0 = \lambda_{\rm c}$ and hence $\tau_A = \omega_{\rm c}^{-1}$ in the calculation below. The numerical calculation is performed on the basis of the Runge-Kutta method with an adaptive time step to gain better calculation precision. The initial position and velocity of the particle are randomly taken within the phase space regime

$$\begin{aligned} &-1.0 < x' < 1.0,\ \ -0.1 < y' < 1.0,\ \ z' = 0.0 \\ &-0.5 < v_x' < 0.5,\ -0.5 < v_y' < 0.5, \\ &-0.5 < v_z' < 0.5, \end{aligned} \tag{9}$$

and the initial time and space steps are taken as $\delta t' = 0.01$ and $|\delta x'| = 0.01$, respectively.

In principle, in the magnetized region of $r' > 1$ the magnetic field is strong enough to conserve the magnetic moment $\mu_{\rm M} = w_\perp/B$ of a particle, where $w_\perp$ is the perpendicular kinetic energy of the particle, and the guiding center of the particle moves at the drift velocity $\boldsymbol{v}_{\rm E} = \boldsymbol{E} \times \boldsymbol{B}/B^2$. In the nonmagnetized region around the X point with $r' < 1$, however, the strong inhomogeneity in the magnetic field breaks conservation of the magnetic moment $\mu_{\rm M}$ of the particle, and the particle undergoes a chaotic orbit and experiences an almost stochastic acceleration and deceleration by the electric field E_z.

Figure 2 shows the projections of the particle orbits onto the x-y plane perpendicular to the guide field, where the parameters $\delta = 0.5$ for the guide field (i.e., $B_z = 0.5B_0$) and $M_{\rm A} = 0.002$ for the electrostatic field (i.e., $E_z = 0.002 v_{\rm A} B_0$) have been used. These orbits can be categorized into three kinds (Gontikakis et al. 2006): (i) mirror-oscillation orbits in the left column in Figure 2 which make mirror oscillations with the majority in the magnetized region and between times skimming through the nonmagnetized region; (ii) magnetized-drift orbits in the middle column in Figure 2 which gradually drift apart from the nonmagnetized region into the magnetized region via the drift motion $\boldsymbol{v}_{\rm E}$; and (iii) chaotic orbits in the right column in Figure 2 which continually pass by the X point in the nonmagnetized region and present obviously orbital randomicity due to scattering by the X point (Numata & Yoshida 2002). Based on the analysis of cluster observations of a magnetotail reconnection event, Wang et al. (2010) found that the lower and higher energetic electrons in the reconnection region have a field-aligned bidirectional velocity distribution and an isotropic velocity distribution, respectively, which can be considered as evidence for the existence of mirror and chaotic motions, respectively.

Figure 3 shows variations of the magnetic moment ($\mu_{\rm M}$) and the distance from the X point (R) corresponding to the particle orbits in Figure 2. From Figure 3, the

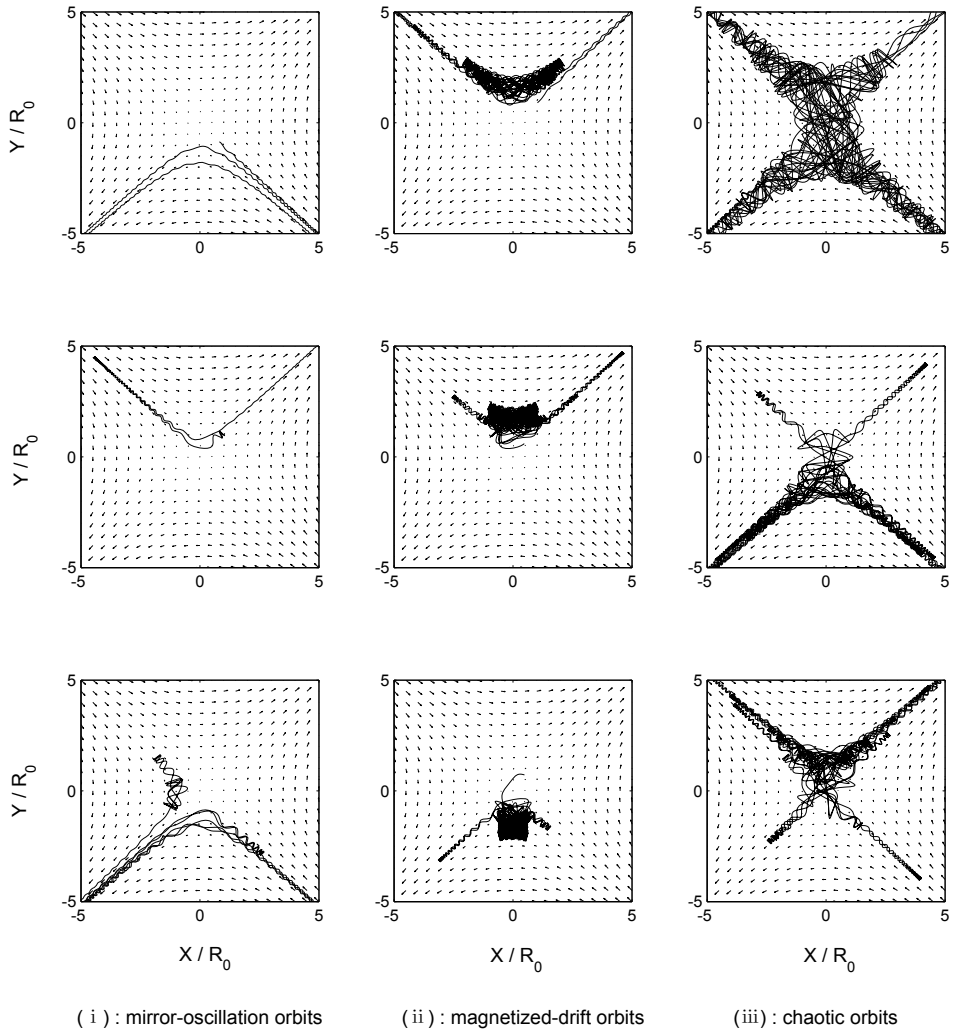

Fig. 2 Three kinds of particle orbits: (i) mirror-oscillation orbits; (ii) magnetized-drift orbits; and (iii) chaotic orbits.

magnetic moment and distance in the mirror-oscillation orbits (the left column) quasi-periodically vary because of the mirror oscillation motion of the particles and variation of the magnetic moment can be attributed to acceleration and deceleration by the electrostatic field E_z during the mirror oscillation. For the case of magnetized-drift orbits in the middle column, the magnetic moment is approximately conserved and the distance slowly increases as the particle gradually drifts apart from the X point as shown in the middle column of Figure 3. For particles with chaotic orbits in the right column in Figure 2, both magnetic moment and distance vary dramatically via stochastic acceleration by the electrostatic field E_z during which they continually skim through the nonmagnetized region and are scattered randomly by the X point.

The degree of stochasticity of individual particle motion on a given orbit can be measured quantitatively by the maximal Lyapunov index of the given orbit in 6-dimensional phase space, which characterizes the average divergence of initially neighboring orbits (Numata & Yoshida 2003).

Figure 4 shows the maximal Lyapunov indices of the corresponding orbits in Figure 2, in which the outermost lines are the one-dimensional maximal Lyapunov index and other lines, from outer to inner, are in turn the differences between the two- and one-dimensional, the three- and two-dimensional, the four- and three-dimensional, the five- and four-dimensional, and the six- and five-dimensional maximal Lyapunov indices. From Figure 4, as expected, the chaotic orbits have Lyapunov indices much larger than those of the mirror-oscillation and magnetized-drift orbits, implying that the randomic-

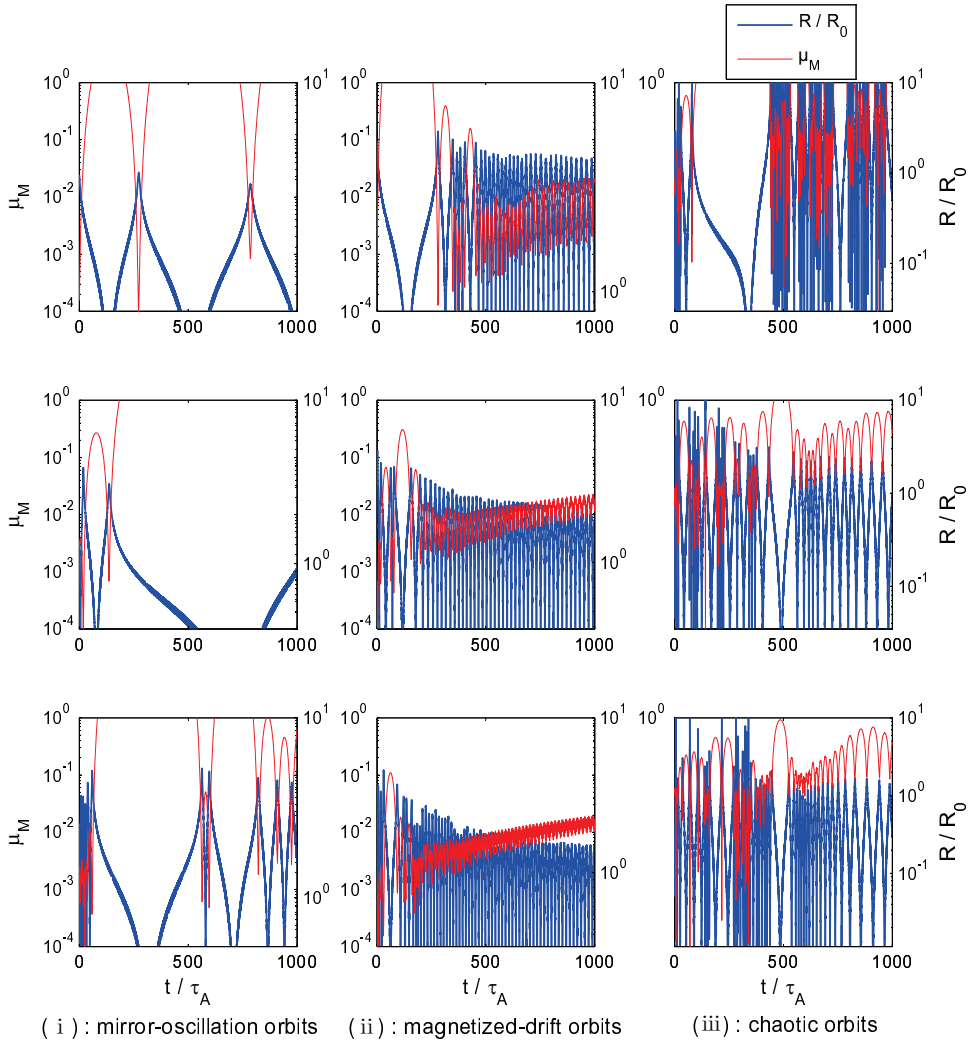

Fig. 3 The variations of the magnetic moment ($\mu_{\rm M}$, *red lines*) and the distance from the X point (R, *blue lines*) of the particles on the orbits shown in Fig. 2.

ity of the chaotic orbits is remarkably higher than that of regular mirror-type and magnetized-drift orbits.

4 STATISTICAL CHARACTERISTICS AND EFFECTIVE RESISTIVITY IN A CURRENT SHEET

In order to study the macroscopic statistical properties of chaotic particle orbits, especially the effective resistivity associated with randomicity of these chaotic orbits, we further simulate the statistical distribution and the kinetic evolution of a multi-particle system by using 2×10^5 particles. The associated initial positions and velocities have uniform distributions in the region $-1.0 < x',\ y' < 1.0$ and $-0.5 < v'_x,\ v'_y,\ v'_z < 0.5$, respectively. Following Numata & Yoshida (2003), we estimate the radius of the chaos region, R_C, based on the temporal stability of the Lyapunov index, that is, the Lyapunov index for the ensemble average orbits of particles within the chaos region does not decrease with the average staying time in the chaos region.

Figure 5 shows the radius of the chaos region increases as the guide field B_z increases for Alfvén Mach numbers $M_{\rm A} = 0.0005$, 0.001, 0.002 and 0.003, which represents acceleration by the electric field $E_z = M_{\rm A} v_{\rm A} B_0$. Moreover, the radius R_C increases faster with the guide field B_z for a larger Mach number $M_{\rm A}$.

The corresponding stable Lyapunov index, on the other hand, decreases as the guide field increases, but does not sensitively depend on Mach number as shown in Figure 6. This indicates that the randomicity of motion of

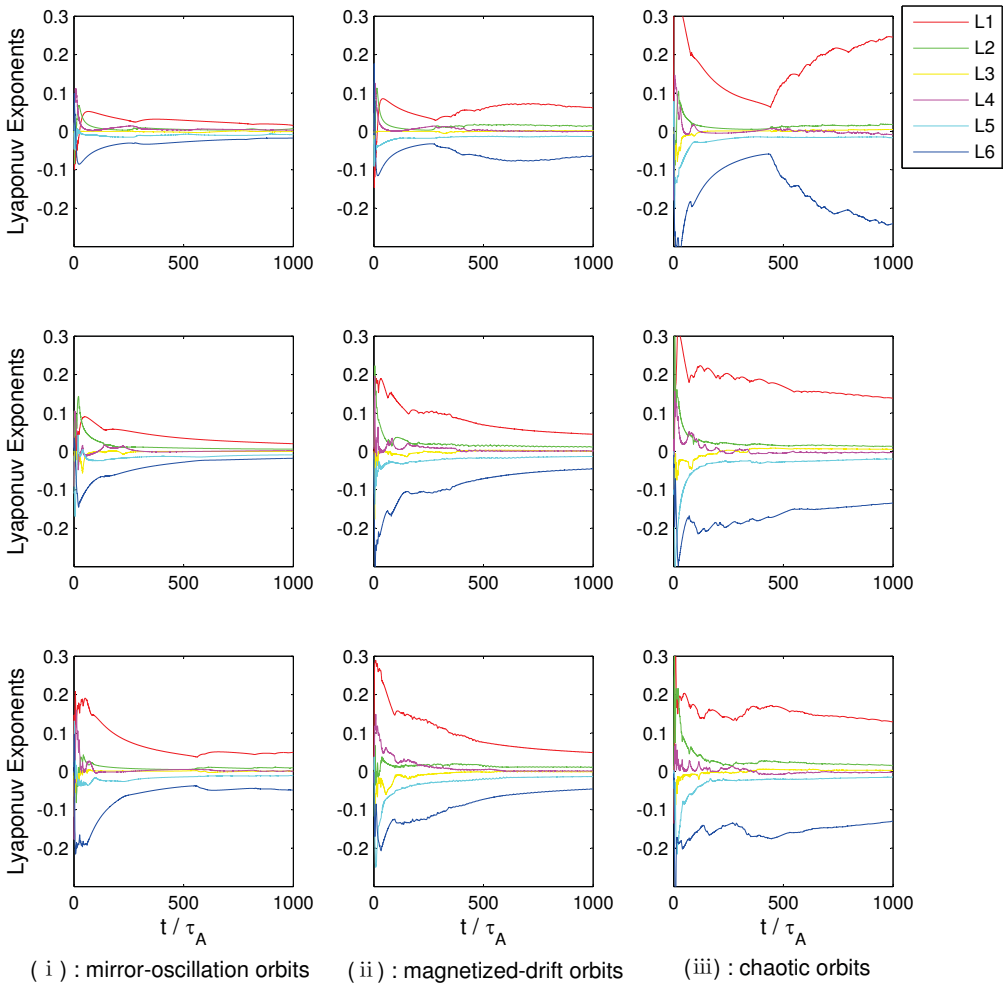

Fig. 4 The Lyapunov indices of the particle orbits shown in Fig. 2.

particles in the chaos region is reduced by the presence of the guide field. One of the possible causes is that the guide field considerably strengthens the magnetic field in the chaos region, and as a result the magnetic gyromotion of particles in the chaos region has a smaller gyroradius and less probability of stochastic scattering by the X point.

Particles in the chaos region are stochastically accelerated by the electric field E_z, and as a result the ensemble average velocity along the guide field, $\bar{v}_z$, increases approximately proportionally to the average staying time in the chaos region $\bar{t}$ (Numata & Yoshida 2003), that is,

$$\bar{v}_z'(\bar{t}') = \alpha \bar{t}'. \tag{10}$$

Figure 7 plots the acceleration coefficient α versus the guide field B_z for acceleration by the given electric field with Mach numbers $M_{\rm A} = 0.0005$, 0.001, 0.002 and 0.003. From Figure 7 the acceleration coefficient α increases considerably with the electric field (i.e., $M_{\rm A}$) as expected, implying that the acceleration of electrons is dominated by the parallel electric field in the presence of the guide field (Wan et al. 2008; Huang et al. 2010). The result presented in Figure 7 also shows that the acceleration coefficient α decreases as the guide field strengthens, implying the guide field can effectively depress the average acceleration the particles in the chaos region. A possible reason is that a stronger guide field leads to a larger chaos region, in which more particles further away from the X point are included in the larger chaos region and their net acceleration efficiency is reduced by the stronger transverse magnetic field perpendicular to the electric field. Moreover, from Figure 7 it can be found that this reduced effect becomes more significant for a stronger electric field and a stronger guide field. It should

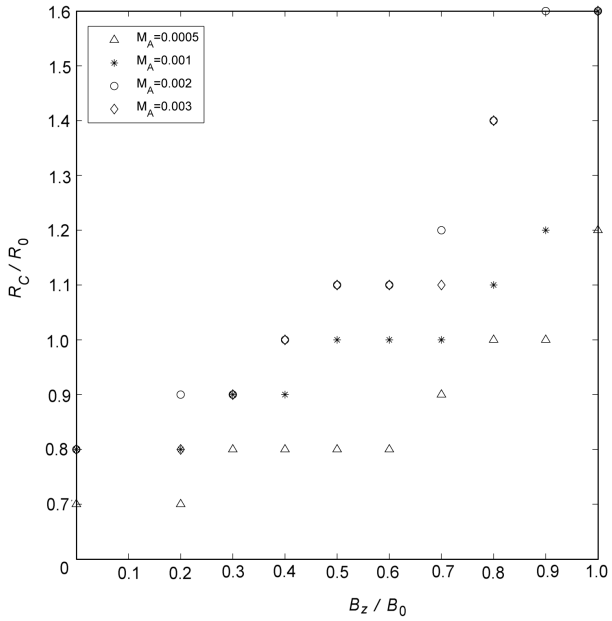

Fig. 5 The radius of the chaos regions R_C versus the guide field B_z, where R_C and B_z are normalized by the characteristic scale of the ambient magnetic field variation R_0 and the characteristic strength of the reconnection field B_0 respectively.

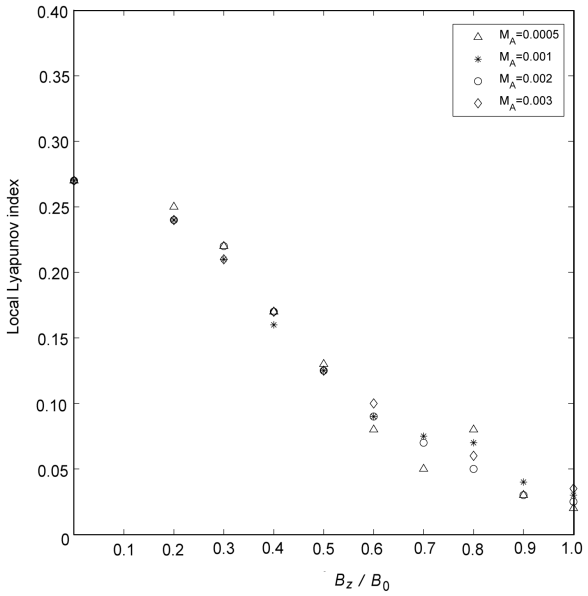

Fig. 6 The Lyapunov indices versus the guide field B_z normalized by B_0.

be pointed out that this result does not contradict the test-particle simulations of Liu et al. (2009), who found that the guide field favors the acceleration of energetic particles for a fixed reconnection region.

It is evident that without supplying new particles the number of particles in the chaos region decreases due to particles escaping from the chaos region. The number of particles in the chaos region decreases approximately exponentially (Numata & Yoshida 2003)

$$n(\bar{t}') = n_0 \exp(-\beta \bar{t}'), \tag{11}$$

and hence the loss rate of particles from the chaos region is

$$\frac{dn(\bar{t}')}{d\bar{t}'} = -n_0 \beta \exp(-\beta \bar{t}') \tag{12}$$

with a loss rate index β. Figure 8 shows the particle loss rate index β versus the guide field for the given electric

field with $M_{\rm A} = 0.0005$, 0.001, 0.002 and 0.003. From Figure 8 the particle loss rate index β increases considerably with the electric field (i.e., $M_{\rm A}$) and this indicates that acceleration by the stronger field leads to particles escaping faster. On the other hand, for the weak guide field of $B_z < 0.5\,B_0$ the loss rate index β increases slightly with the guide field strength. For the guide field of $B_z > 0.5\,B_0$, however, the loss rate index considerably decreases as the guide field increases, especially for the case of acceleration from the strong field with $M_{\rm A} > 0.001$.

To estimate the effective resistivity for a steady condition in equilibrium, Numata & Yoshida (2003) proposed considering a sustained system, in which the total number of particles is conserved through supplying new particles with zero average velocity. When including the acceleration of new particles using Equation (10), under the steady, equilibrium case, such a sustained system has a steady ensemble-average velocity

$$\bar{v}_0' = \frac{\alpha}{\beta}. \tag{13}$$

On the other hand, a steady, equilibrium case can be reached when the electrostatic force by the electric field eE_z is balanced by an effective collision resistance $\nu_{\rm eff} v_z$ with the effective collision frequency $\nu_{\rm eff}$, and the resulting steady velocity may be obtained as follows

$$\bar{v}_0' = \frac{M_{\rm A} E_z'}{\nu_{\rm eff}} = \frac{M_{\rm A}}{\nu_{\rm eff}}. \tag{14}$$

Comparing Equations (13) and (2) leads to the effective collision frequency

$$\nu_{\rm eff} = \frac{\beta}{\alpha} M_{\rm A}. \tag{15}$$

Figure 9 presents the effective collision frequency versus the guide field for the electric field with Mach numbers $M_{\rm A} = 0.0005$, 0.001, 0.002 and 0.003. The result displayed in Figure 9 demonstrates that, as shown by Equation (15), the effective collision frequency $\nu_{\rm eff}$ and hence the chaos-induced resistivity increases considerably with the electric field because acceleration by the stronger electric field requires a larger resistance to balance the higher chaos-induced resistivity. For the weak guide field of $B_z < 0.5\,B_0$, $\nu_{\rm eff}$ increases with guide field strength because the loss rate index β increases. For a guide field of $B_z > 0.5\,B_0$, however, the effective collision frequency considerably decreases as the guide field increases. This is consistent with the result of particle-in-cell simulations by Pritchett & Coroniti (2004); Fu et al. (2006); Wan et al. (2008); Huang et al. (2010), who found that the reconnection rate may be largely reduced

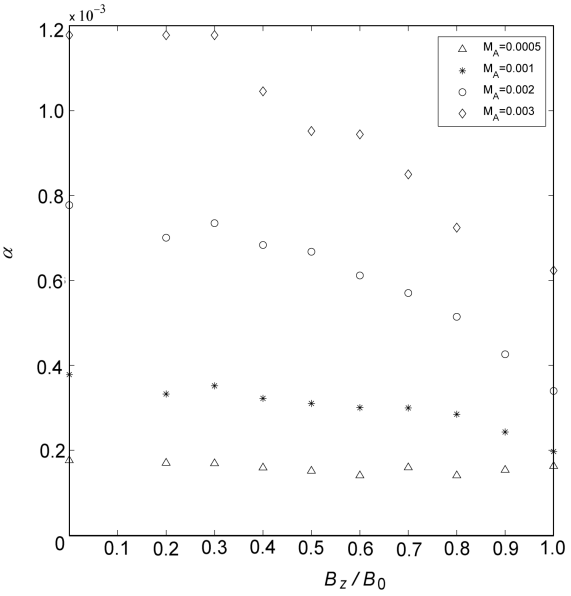

Fig. 7 The acceleration coefficient α versus the guide field B_z for the given electric field E_z with Mach numbers $M_{\rm A} = 0.0005$, 0.001, 0.002 and 0.003.

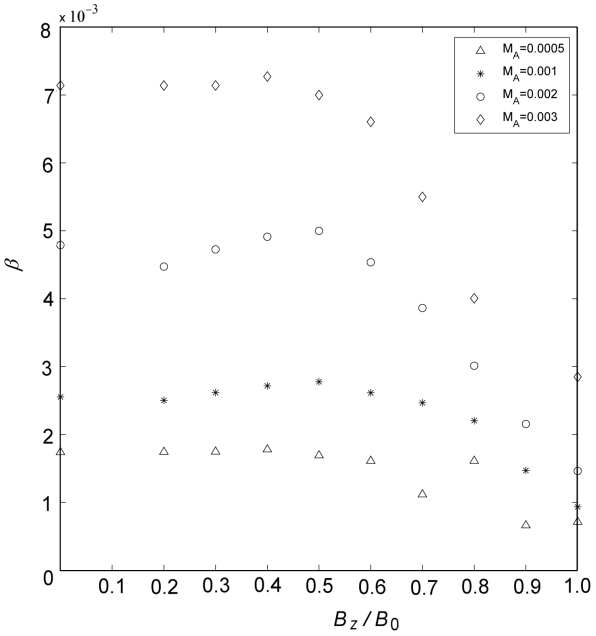

Fig. 8 The loss rate index β versus the guide field B_z for the given electric field E_z with the Mach numbers $M_{\rm A} = 0.0005$, 0.001, 0.002 and 0.003.

for the case of a large guide field of $B_z > B_0$. In particular, the effective collision frequency and hence the chaos-induced resistivity reaches its peak value near the guide field approaching one half of the characteristic strength of the ambient reconnection field, that is, $B_z \sim 0.5\,B_0$.

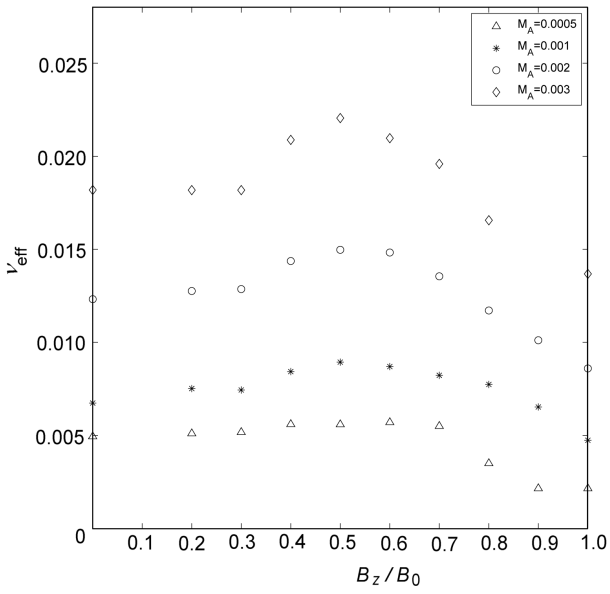

Fig. 9 The effective collision frequency $\nu_{\rm eff}$ versus the guide field B_z for the given electric field E_z with Mach numbers $M_{\rm A} = 0.0005$, 0.001, 0.002 and 0.003.

This results from competition between the chaos region scale and the local Lyapunov index, which increases and decreases, respectively, with the guide field as shown in Figures 5 and 6.

5 SUMMARY AND CONCLUSIONS

Magnetic reconnection is now believed to be largely responsible for the energy release in various astrophysical eruptive phenomena. However, the generation mechanism of anomalous resistivity in magnetic reconnection has been an open and puzzling problem. Numata & Yoshida (2002) pointed out that the magnetic null point in the reconnecting current sheet can act as a scattering center and lead to chaotic motions of particles in the current sheet. They proposed that this chaos possibly contributes to the formation of anomalous resistivity, called chaos-induced resistivity. In many interesting cases, however, instead of the magnetic null point, there is a nonzero magnetic field perpendicular to the merging field lines, that is, the so-called guide field.

Taking account of the effect of this nonzero guide field, by use of the particle simulation method, we calculate the particle orbits in the magnetic reconnection region. The result shows that although the dynamic orbits of the particles differ widely and show great complexity, the majority of them can conform to one of the following three kinds: the mirror-oscillation orbit, the magnetized-drift orbit and the chaotic orbit. Analysis of the Lyapunov index of these particle orbits, which represents the degree of particle motion stochasticity, indicates that the contribution to the anomalous resistivity comes mainly from the chaotic orbits. In order to study the contribution of these particle chaotic orbits on anomalous resistivity, we further simulate the statistical distribution and its evolving properties of a multi-particle system by using 2×10^5 particles. The results show that the radius of the chaos region increases with the guide field but the Lyapunov index decreases with the guide field. However, the effective collision frequency, and hence the chaos-induced resistivity, has its peak value near $B_z = 0.5\, B_0$ (i.e., the guide field is one half of the reconnection field).

The anomalous resistivity is an important parameter, and plays a key and deciding role in magnetic energy release, especially in the collisionless reconnection rate. The present result is helpful for us to understand the microphysics of anomalous resistivity in the case of collisionless reconnection with a guide field.

Acknowledgements Research by DJW and MS was supported by the National Natural Science Foundation of China (NSFC, Grant Nos. 41531071 and 11373070), LC was supported by the NSFC (Grant No. 41304136) and by the Key Laboratory of Solar Activity at National Astronomical Observatories (Grant KLSA 201502), and PFC was supported by the NSFC (Grant Nos. 11025314 and 11533005).

References

Biskamp, D., Schwarz, E., & Drake, J. F. 1995, Physical Review Letters, 75, 3850

Boozer, A. H. 1986, Journal of Plasma Physics, 35, 133

Bulanov, S. V., Pegoraro, F., & Sakharov, A. S. 1992, Physics of Fluids B, 4, 2499

Dungey, J. W. 1958, in IAU Symposium, 6, Electromagnetic Phenomena in Cosmical Physics, ed. B. Lehnert, 135

Dungey, J. W. 1961, Physical Review Letters, 6, 47

Egedal, J., & Fasoli, A. 2001, Physical Review Letters, 86, 5047

Fitzpatrick, R., & Porcelli, F. 2004, Physics of Plasmas, 11, 4713

Fu, X. R., Lu, Q. M., & Wang, S. 2006, Physics of Plasmas, 13, 012309

Giovanelli, R. G. 1946, Nature, 158, 81

Gontikakis, C., Efthymiopoulos, C., & Anastasiadis, A. 2006, MNRAS, 368, 293

Grad, H., & Van Norton, R. 1962, Nucl. Fusion Suppl., 1, 61

Horton, W., Liu, C., Hernandez, J., & Tajima, T. 1991, Geophys. Res. Lett., 18, 1575

Huang, C., Lu, Q., & Wang, S. 2010, Physics of Plasmas, 17, 072306

Huba, J. D., Drake, J. F., & Gladd, N. T. 1980, Physics of Fluids, 23, 552

Liu, W. J., Chen, P. F., Ding, M. D., & Fang, C. 2009, ApJ, 690, 1633

Lyutikov, M. 2006, MNRAS, 369, L5

Numata, R., & Yoshida, Z. 2002, Physical Review Letters, 88, 045003

Numata, R., & Yoshida, Z. 2003, Phys. Rev. E, 68, 016407

Parker, E. N. 1957, J. Geophys. Res., 62, 509

Pritchett, P. L., & Coroniti, F. V. 2004, Journal of Geophysical Research (Space Physics), 109, A01220

Ricci, P., Brackbill, J. U., Daughton, W., & Lapenta, G. 2004, Physics of Plasmas, 11, 4102

Schmidt, G. 1962, Physics of Fluids, 5, 994

Spitzer, L. 1956, Physics of Fully Ionized Gases (New York: Interscience Publishers)

Sweet, P. A. 1958, in IAU Symposium, 6, Electromagnetic Phenomena in Cosmical Physics, ed. B. Lehnert, 123

Wan, W., Lapenta, G., Delzanno, G. L., & Egedal, J. 2008, Physics of Plasmas, 15, 032903

Wang, R., Lu, Q., Huang, C., & Wang, S. 2010, Journal of Geophysical Research (Space Physics), 115, A01209

Yoshida, Z., Asakura, H., Kakuno, H., et al. 1998, Physical Review Letters, 81, 2458